Microfluidics and Nanofluidics (2019) 23:21
https://doi.org/10.1007/s10404-018-2179-5

RESEARCH PAPER

Double-line particle focusing induced by negative normal stress difference in a microfluidic channel

Sei Hyun Yang[1] · Doo Jin Lee[2] · Jae Ryoun Youn[1] · Young Seok Song[3]

Received: 4 September 2018 / Accepted: 14 December 2018 / Published online: 17 January 2019

Abstract

Particles suspended in diluted viscoelastic fluids migrate in the transverse direction of the fluid flow towards equilibrium locations determined by spatial normal stress distributions across the cross-section of microfluidic channels. Polymer solutions with a negative first normal stress difference exhibit unexpected fluid behaviors such as material contraction after die extrusion and filament compression of semiflexible biopolymer gels in abrupt shear flow. The lateral particle migration was investigated in a hydroxypropyl cellulose (HPC) viscoelastic fluid with a negative first normal-stress difference. Unlike common viscoelastic fluids with positive normal stress differences, double-line particle focusing was identified in a microfluidic channel, which was caused by the negative first normal stress difference. More importantly, unique particle migration with different-sized particles in a microchannel was observed in which bigger particles were double-line focused along the channel walls while smaller particles were single-line focused at the center. A new particle focusing mechanism was suggested to demonstrate this unique double line focusing behavior of particles in the viscoelastic fluids.

Keywords Negative first normal-stress difference · Viscoelastic particle focusing · Normal stress component · Hydroxypropyl cellulose

1 Introduction

Particle handling based on the viscoelastic fluid is an emerging technique that has been developed over the past 10 years owing to its simplicity and high-quality focusing in a wide range of flow rates (Yang et al. 2011, 2017; D'Avino et al. 2012; Romeo et al. 2013; Del Giudice et al. 2013, 2015a; Kang et al. 2013; Lee et al. 2013; Lim et al. 2014a, b; Ahn et al. 2015; Yuan et al. 2015; Howard et al. 2015; Kim and Kim 2016). Since an early experimental work by Leshansky et al. (2007) introduced the particle focusing in a slit channel that is due to an imbalance among the normal stresses imposed onto particles, the particle-focusing behavior in viscoelastic fluids has received substantial interest and widely been studied (Huang et al. 1997; Leshansky et al. 2007; Yang et al. 2011; Kang et al. 2011; D'Avino et al. 2012; Young Kim et al. 2012; Del Giudice et al. 2013, 2015a; Lee et al. 2013; Lim et al. 2014a, b; Yuan et al. 2015; Kim and Kim 2016). Later, Yang et al. (2011) demonstrated the particle focusing in viscoelastic fluids at the centerline of a square channel and four corners depending on the combination of the fluid elasticity and inertia. The viscoelasticity-induced particle migration can be realized even when the

Sei Hyun Yang and Doo Jin Lee are equally contributed to this study.

This article is part of the topical collection "Particle motion in non-Newtonian microfluidics" guest edited by Xiangchun Xuan and Gaetano D'Avino.

✉ Jae Ryoun Youn
jaeryoun@snu.ac.kr

✉ Young Seok Song
ysong@dankook.ac.kr

[1] Research Institute of Advanced Materials (RIAM), Department of Materials Science and Engineering, Seoul National University, Seoul 08826, Republic of Korea

[2] Ceramic Fiber and Composite Materials Center, Korea Institute of Ceramic Engineering and Technology, 101 Soho-ro, Jinju-si, Gyeongsangnam-do 52851, Republic of Korea

[3] Department of Fiber System Engineering, Dankook University, Yongin, Gyeonggi-do 16890, Republic of Korea

Reynolds number (*Re*) approaches zero due to the presence of elastic stresses.

The viscoelasticity-induced particle-focusing technique is beneficial in a variety of analytical and processing applications such as sorting of particles (Yang et al. 2011; Young Kim et al. 2012; Cartas-Ayala et al. 2013; Guan et al. 2013; Kang et al. 2013; Liu et al. 2015; Lu and Xuan 2015; Lu et al. 2015; Nam et al. 2015), fluid transportation around particles (Li et al. 2015), measurement of the relaxation times of viscoelastic fluids (Del Giudice et al. 2015b), and efficient trapping and stretching of particles at a stagnation point (Cha et al. 2012; Kim et al. 2017). In more detail, an enhanced flow-asymmetry fluid transport around particles was demonstrated using the Giesekus fluids (Li et al. 2015). A chip-based rheometry was also developed by harnessing the focusing behavior of particles to estimate the relaxation time of viscoelastic fluids (Del Giudice et al. 2015b). The chip-based rheometry enabled the measurement of relaxation time at the millisecond level without requiring a calibration curve employed in conventional tests. Also, cell stretching in the microfluidic device was analyzed with use of the viscoelasticity-induced cell focusing and trapping at the stagnation point of the cross-slot channel (Cha et al. 2012; Kim et al. 2017). In contrast to the inertial particle-focusing method, the particle-focusing method using viscoelasticity can prevent a random lateral cell distribution and then guarantee rotation-free cell stretching along the channel centerline.

Ho and Leal (1976) initiated a theoretical work to understand the lateral-migration mechanism of particles in viscoelastic fluids, in which the migration of particles in a second-order fluid was caused by the spatial gradient of the first normal stress difference, defined as $N_1 = \tau_{xx} - \tau_{yy}$. Here, τ_{xx} and the τ_{yy} are the normal-stress components in the flow- and velocity-gradient directions, respectively. The particle migration in the pressure-driven flow of viscoelastic fluids has been simulated considering a wide range of factors such as the effect of inertia and elasticity, the shear-thinning viscosity, the secondary flow, and the blockage ratio (D'Avino et al. 2012; Villone et al. 2013; Li et al. 2015). For most viscoelastic polymer solutions, the magnitude of the second normal-stress difference $N_2 = \tau_{yy} - \tau_{zz}$, which produces a secondary flow over the channel cross-section, is much smaller than that of N_1, where the τ_{zz} is the normal-stress component in the rotational direction (Barnes 1989).

The viscoelasticity-induced focusing of particles in slit flow and square-channel flow was modeled by means of three-dimensional (3D) finite-element simulation (Villone et al. 2011, 2013). The simulation results showed that the particles migrated toward the channel centerline or the closest corners depending on the initial particle positions. A single dimensionless number that can help explain the migration dynamics of a particle in viscoelastic fluids at the low Deborah number was proposed to offer a guideline for the particle focusing (Del Giudice et al. 2013; Romeo et al. 2013). In addition, a potential energy concept was recently introduced by considering the integration of a net-lift force composed of elastic and inertial forces acting on the particles (Tian et al. 2017). Typically, it is assumed that τ_{xx} is much larger than τ_{yy} in most complex fluids, resulting in a positive N_1. Interestingly, some complex fluids such as liquid-crystal polymer solutions (Kiss and Porter 1980) and nanotube suspensions (Lin-Gibson et al. 2004) exhibit a negative N_1. For example, carbon nanotube-filled polymer shows unusual contraction properties after die extrusion due to the negative N_1 (Kharchenko et al. 2004; Pasquali 2004). The networks of semiflexible biopolymer gels constituting the cytoskeleton of cells and extracellular matrix also induce the compression of filament in an orthogonal direction to the shear direction (Janmey et al. 2007). This study aims at investigating the particle migration in viscoelastic fluids with the negative N_1. Based on our experimental results, we confirm that the particles in the viscoelastic fluid with the negative N_1 migrates in the opposite direction to the case with the positive N_1. Furthermore, the particles suspended in the viscoelastic solution with the negative N_1 show an opposite focusing behavior compared with those in the solution with the positive N_1. We propose a possible migration mechanism to explain the movement of particles in a microfluidic channel.

2 Materials and methods

The microchannels employed in this study were replicated using a standard soft-lithography method. Straight microfluidic channels with a channel aspect ratio ($AR = W:H$) of 2 were fabricated. A poly(dimethylsiloxane) (PDMS) was mixed with a curing agent and poured onto an SU-8 master mold. After the prepolymer was degassed in a vacuum chamber for 1 h, it was cured at 70 °C for 4 h. The PDMS channel was peeled off and punched with a 1.5-mm-diameter puncher (Harris Uni-Core, Sigma-Aldrich, USA), enabling the connection of the tubes to reservoirs. The channel was bonded onto a slide glass using a plasma-treatment device (BD-10A, Electro-Technic Products Inc., USA), and then heated at 120 °C for 1 h to enhance the bonding strength.

Two kinds of polymers were dissolved into 22 wt% aqueous glycerol solution to prepare dilute polymer solutions for experiments. Polyethylene oxide (PEO) solutions with the molecular weight of 2,000,000 and hydroxypropyl cellulose (HPC) solution with the molecular weight of 1,000,000 were purchased from Sigma-Aldrich (USA), which have a positive N_1 and a negative N_1 due to the unique liquid-crystal structures, respectively (Fried et al. 1994; Martins et al. 2001; Hoekstra et al. 2002; Kulichikhin et al. 2011). Both diluted PEO and HPC

solutions were prepared with various polymer concentrations in the range of 100–4000 ppm to investigate the lateral particle migration in the microchannel. Polystyrene (PS) particles (Polysciences, USA) with diameters of 5, 10, and 15 μm and fluorescent PS particles (Polysciences, U.S.A.) with a 6.42 μm diameter were suspended in the viscoelastic mediums. A small amount of the surfactant, P1379-25ML TWEEN 20 (Sigma-Aldrich, USA), was used to prevent the particle aggregation. The diluted polymer solutions were injected into the microchannel using a syringe pump (KDS 200, KD Scientific, USA) with flow rates ranging from 0.1 to 2.5 ml/h. An inverted optical microscope (IX 53, Olympus America Inc., USA) and a vision-hi charge-coupled device (CCD) camera (AcquCAM 23G, JNOpTIC Co. Ltd., South Korea) were used to observe the particle migration in the viscoelastic fluids. The particle-focusing behaviors were analyzed using the Image-Pro Plus (Media Cybernetics, Inc., USA) and ImageJ (National Institutes of Health, USA) image-processing software packages.

2.1 Rheological properties of the viscoelastic solutions

The rheological properties of the diluted PEO and HPC solutions were measured using a standard rotational rheometer (MCR 302, Anton Paar, Germany). The steady-shear viscosities were determined using a double-gap geometry (Fig. 5b). The rheological characteristics of the diluted PEO and HPC solutions are different due to the different molecular structures and responses to the applied flow. In particular, the HPC molecules in the solution tend to align along the flow direction similar to liquid crystals (Hongladarom et al. 1994; Phillies et al. 2003; Kulichikhin et al. 2011). As a result, the HPC molecules can generate a negative N_1. The origin of the negative N_1 is unclear, although it has been linked with a flow induced molecular orientation and a phase separation in the direction perpendicular to the flow (Pasquali 2004). The N_1 of the viscoelastic solution was generally measured using a cone and plate geometry with 50 mm diameter. The normal force F_N acting on the upper cone was measured as follows.

$$F_N = \frac{\pi R^2}{2}\left[\tau_{xx} - \tau_{yy}\right] = \frac{\pi R^2}{2} N_1 \tag{1}$$

In addition, the difference between the first and second normal stress differences was obtained by measuring the normal force with a parallel plate geometry.

$$\Delta N = N_1 - N_2 = \tau_{xx} - 2\tau_{yy} + \tau_{zz} = \frac{2F}{\pi R^2}\left[1 + \frac{d\ln F}{2d\ln \Omega}\right], \tag{2}$$

where N_2 is the second normal-stress difference, R is the radius of the parallel plate, and Ω is the angular velocity (Morrison 2001; Shaw and MacKnight 2005) and τ_{yy} is the normal stress in the transverse direction to the shear-flow direction, i.e., the velocity-gradient direction (Miller and Christiansen 1972; Morrison 2001; Shaw and MacKnight 2005).

According to Zimm's theory for polymer solutions, the relaxation time of polymers is dependent on the structural characteristics. It is expressed as $\lambda_{\text{zimm}} \approx \frac{\mu_s R_g^3}{k_B T}$, where μ_s is the solution viscosity, k_B is the Boltzmann's constant, T is the absolute temperature, and R_g is the radius of the gyration of an entangled polymer chain. In this study, the R_g of HPC ($M_w = 1{,}000{,}000$) in the solution was approximately 124 ± 24 nm, which is much larger than that of the PEO ($M_w = 2{,}000{,}000$), i.e., $R_g \sim 65$ nm (Acad 1984; Korneeva et al. 1990; Procedures 1990; Phillies et al. 2003; Kang et al. 2013; Eom et al. 2016). Since the relaxation time of the diluted HPC solution is very small, it is difficult to measure it with a conventional capillary breakup extensional rheometer. Therefore, Zimm's theory for the estimation of the relaxation time was employed and the relaxation time was compared with that of the Carreau–Yasuda model (see Table 1). In the case of the diluted PEO solution, however, the relaxation time can be measured using a capillary breakup extensional rheometry. For the measurement, the HAKKE CaBER-1 device (Thermo Fisher Scientific Inc., USA) was used. The relaxation time of the diluted PEO solutions is listed in our previous study (Yang et al. 2017). The relaxation times of both the diluted HPC and PEO solutions were used to calculate the elasticity number El. In viscoelastic fluids, the El is defined as $El = W_i/Re$, which is the ratio of the Weissenberg number ($Wi = N_1/\tau_{xy} = 2\mu\lambda\dot{\gamma}^2/\mu\dot{\gamma} = 2\lambda Q/\text{HW}^2$) to the Reynolds number ($Re = \rho \text{UD}_h/\mu$). In this study, to compare the Wi numbers of the diluted HPC solutions with those of the diluted PEO solutions, the Wi is simply assumed to be $Wi = |N_1|/\tau_{xy}$ in this study. Here, $D_h = 2WH/(W+H)$ is the hydraulic diameter of the rectangular channel, μ is the solution viscosity, λ is the solution relaxation time, and Q is the flow rate.

Table 1 Power law indices and relaxation times of HPC solutions fitted with the Carreau–Yasuda model and Zimm's theory

Polymer concentration [ppm]	Carreau–Yasuda model		Zimm's theory
	n	λ_{mean} (s)	λ_{mean} (s)
100	0.9864	0.00535	0.00879
250	0.9435	0.00857	0.01015
500	0.9232	0.00919	0.01386
750	0.9087	0.01218	0.02248
1000	0.8933	0.01754	0.02565

3 Results and discussion

The particles in the viscoelastic fluid under the confined Poiseuille flow were placed at the center and the four corners of the cross-section of the microchannel as a result of the balance between the elastic and inertial forces. In many cases, diluted PEO and poly(vinyl-pyrrolidone) (PVP) solutions with the positive N_1 are used for viscoelasticity-induced particle focusing. The N_1 is considered as a main factor for the particle migration induced by the elastic force $F_E \sim a^3 \nabla N_1$ (Leshansky et al. 2007; Yang et al. 2011). It is usually assumed that the N_1 is positive since τ_{xx} is much larger than τ_{yy} for common polymer solutions. Thus far, viscoelasticity induced particle focusing in a microfluidic device has been explained using the N_1, but the underlying physics has yet to be understood. For instance, while each normal stress component in the viscoelastic flow plays a key role in determining the particle movement in the channel, the effect of the normal stress component has not been addressed. In this sense, this study investigates how each normal stress component affects the particle focusing based on a force balance principle. It is surprising that polymer solutions with the negative N_1 show unexpected behaviors such as material contraction upon the confinement release (Kharchenko et al. 2004; Pasquali 2004; Janmey et al. 2007). Some polymer melt solutions have negative first normal stress difference such as molten liquid crystalline polymers (LCPs) and carbon nanotube-filled molten nanocomposites. The observation of negative first normal stress difference is a remarkable phenomenon. The origin of the negative first normal stress difference in LCPs and molten carbon nanotube-filled nanocomposites is different and remains unresolved. One of the possible idea for the negative first normal stress difference of LCP is a competition between flow-induced orientation and ordering into a thermodynamically driven nematic state (Larson 1990). In this study, we used water-soluble liquid crystalline polymer, Hydroxypropyl cellulose (HPC), to investigate a particle migration behavior in a viscoelastic solution with negative first normal stress difference and this study is the first exploration dealing with a particle migration in a viscoelastic fluid with negative first normal stress difference. Interestingly, unusual particle-focusing behaviors were observed in the diluted HPC solutions as shown in Fig. 1.

In the experiment, the particles suspended in the Newtonian fluid, the diluted PEO solution, and the diluted HPC solution were supplied randomly into the microfluidic inlet channel. Upon the occurrence of the flow with large inertia ($Re \sim 18.506$), the particles in the Newtonian fluid were randomly distributed throughout the channel. The particles in the 2000 ppm PEO solution showed the center-line particle focusing in the channel, which has been reported in the literature (Yang et al. 2011; D'Avino et al. 2012; Del Giudice et al. 2013, 2015a; Villone et al. 2013). For the 100 ppm HPC solution, the particles were focused at the double-equilibrium positions close to the channel walls. This result is a very unexpected and unique phenomenon which is caused by viscoelasticity rather than channel geometry. The diluted HPC and PEO solutions with various concentrations were prepared, and the N_1 and the first normal stress coefficient $\Psi_1 = (\tau_{xx} - \tau_{yy})/\dot{\gamma}^2$ were measured to explore the effect of the fluid elasticity on the particle-migration mechanism as shown in Fig. 2a and b. The diluted PEO and HPC solutions showed the positive and negative Ψ_1, respectively. The

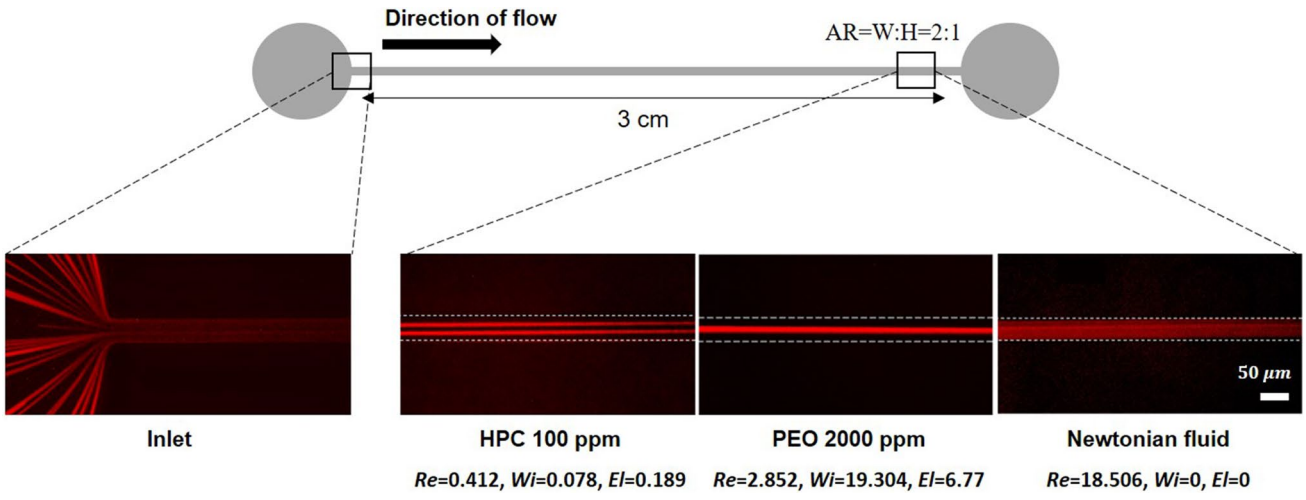

Fig. 1 Particle focusing behavior of solutions. Particle focusing behavior in the straight channel. The particles are double-line focused in the HPC solution with a negative N_1, whereas typical single-line focusing is observed in the PEO solution with a positive N_1. The particles in the Newtonian fluid are randomly distributed

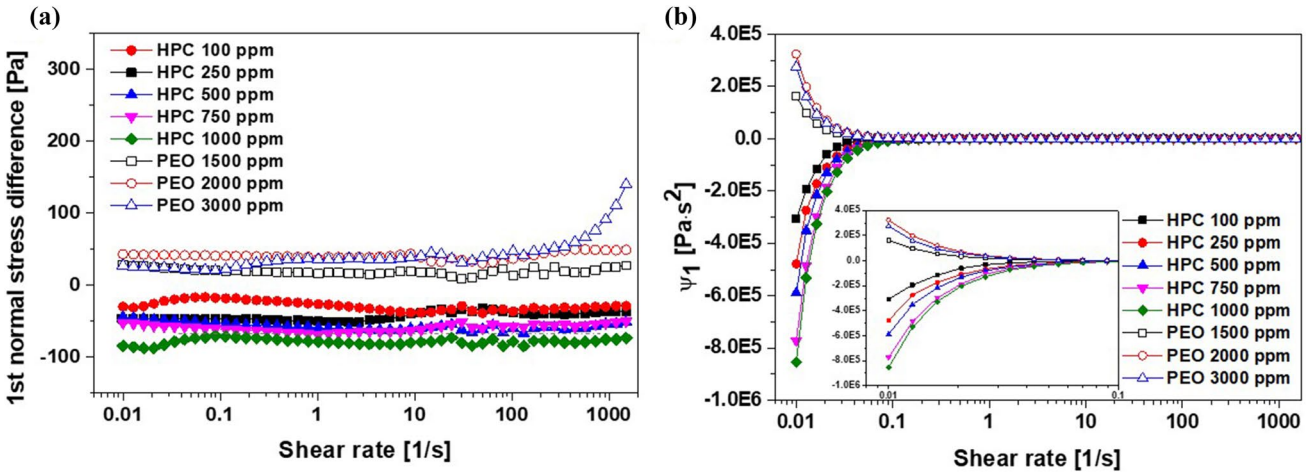

Fig. 2 Rheological properties of PEO and HPC solutions. **a** Measured first normal stress difference (N_1) and **b** first normal stress difference coefficient of HPC and PEO solutions using a bulk rheometer with cone and plate accessary ($d = 50$ mm). HPC solutions have a negative sign of N_1 and PEO solutions have a positive sign of N_1.

magnitude of the negative N_1 value for the HPC solution was increased with an increase in the polymer concentrations. Indeed, this finding enabled us to look into the mechanism of particle migration from a different perspective.

The viscoelasticity-induced particle focusing was analyzed using particles with different diameters of 5, 10, and 15 μm in the diluted HPC solutions and 2000 ppm PEO solution (Fig. 3). The channel-blockage ratio ($\beta = a/H$) is a critical factor for the particle-focusing behavior in viscoelastic fluids. The critical value of β was 0.2 according to the literature. The particles with $\beta \geq 0.2$ in the diluted PEO solutions were focused at the center, whereas the particles with $\beta < 0.2$ moved downstream randomly (Lim et al. 2014b). This technique was used to achieve size-selective particle separations (Kang et al. 2013; Lim et al. 2014b; Lu et al. 2015; Li et al. 2016). In the diluted HPC solutions, the particle motion was different from that in the diluted PEO solutions as shown in Fig. 3. In the figure, one hundred

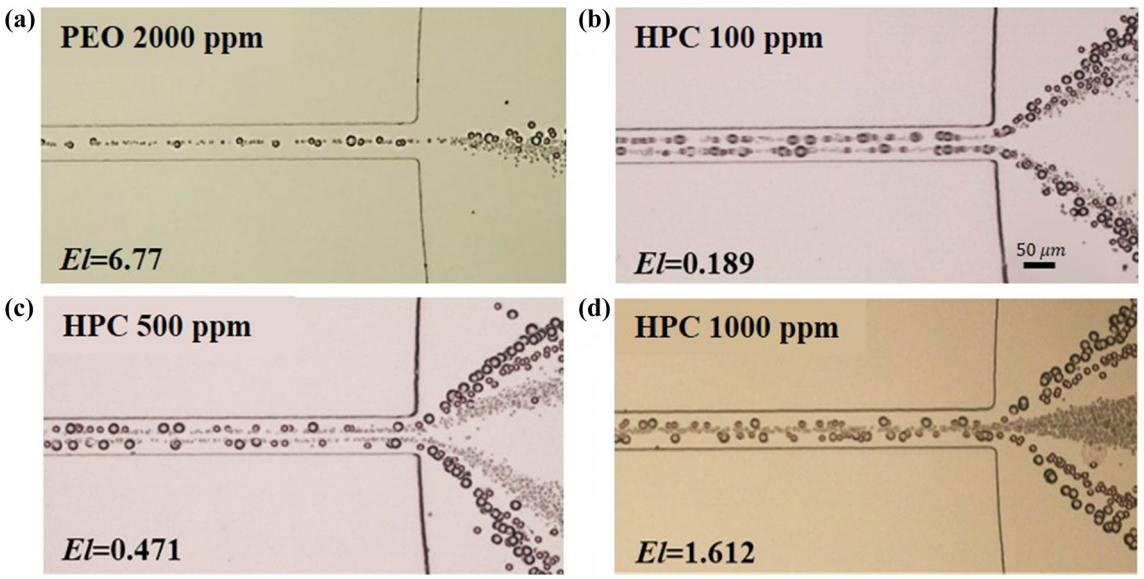

Fig. 3 Particle focusing behavior in HPC solutions with a negative N_1. Microscopic images of the particle focusing in the channel. **a** Typical focusing behavior in PEO solution. **b–d** The reverse particle focusing phenomenon is observed. At the relatively low polymer concentration, all the particles are double-line focused close to the channel walls. However, as the polymer concentration is increased, the large particles are double-line focused, but the small particles are focused at the center. Hundreds of images are superimposed for an enhanced observation of the particle migration

images were superimposed for better observation of the lateral migration of the particles in the 100, 500, and 1000 ppm HPC solutions. The 5, 10, and 15 μm particles in the diluted 100 ppm HPC solutions showed the double-line particle focusing even at low *El* values (Fig. 3b–d). It turned out that the double-line particle-focusing behavior in the HPC solutions strongly depended on the polymer concentration. When the concentration of the HPC solutions was 100 ppm, the double-line particle focusing was clearly observed for all the particles. In this case, it was found that the shear-thinning effect was negligible (please see Fig. 5b and Table 1). For the 5 μm particles, the distance between the two focusing lines was relatively short, and the particles tended to move toward the channel center as the concentration of the HPC solution was increased from 100 to 1000 ppm (Fig. 4a). For the particles of 10 and 15 μm diameters, the double-line focusing was generated close to the side walls of the channel regardless of the HPC concentration. That is, the small

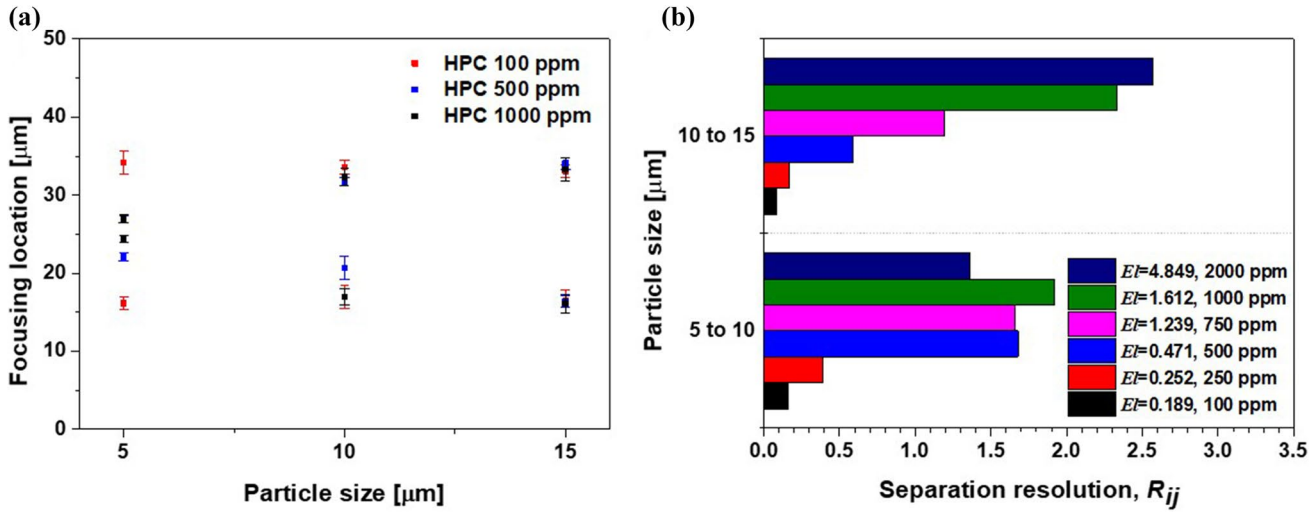

Fig. 4 Particle separation in a straight channel. **a** In 1000 ppm, focusing locations of each particle (5, 10, 15 μm) are analyzed by Image-Pro software. Larger particles are aligned near the channel wall that is closer than the small particles. **b** Particle separation resolution (R_{ij}) of various concentrations is calculated with the relation, $R_{ij} = \Delta x_{ij}/(s_i + s_j)$, where Δx_{ij} is the distance between i and j particle, and s_i is the standard deviation of i particle location

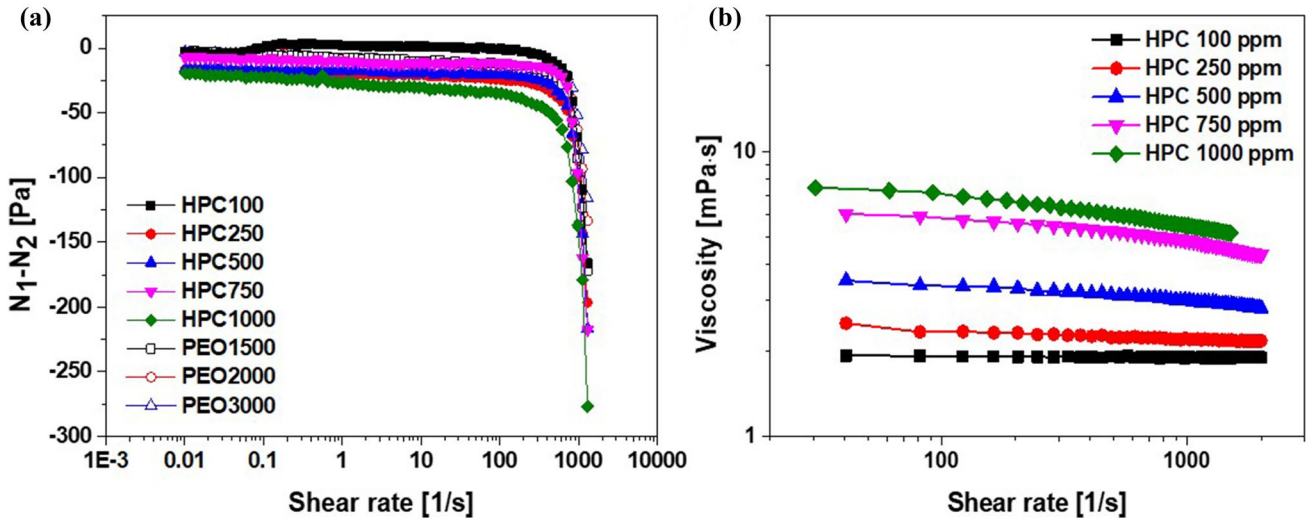

Fig. 5 Viscosities of HPC solution and comparison of HPC and PEO solution regarding normal stress component. **a** $N_1 - N_2$ of each solution is measured using a bulk rheometer with parallel plates accessory ($d = 50$ mm). **b** Viscosities of diluted HPC solutions with different concentrations ranging from 100 to 1000 ppm. The 100 ppm HPC solution possesses a negligible shear thinning effect and the shear thinning effect becomes obvious with increasing the HPC concentrations

particles were focused at the center, while the large particles were double-line focused close to the walls, which is completely different from the literature previously reported.

To demonstrate the particle-sorting efficiency, the particle-separation resolution $R_{ij} = \Delta x_{ij}/(s_i + s_j)$ was calculated with respect to the particle size and the elasticity number, where Δx_{ij} is the distance between the i-th and j-th particles, and s_i is the standard deviation of the i-th particle's location (Kang et al. 2013). The particle-separation resolution showed the highest values at the 1000 ppm HPC solution using the 5 and 10 μm particles and at the 2000 ppm HPC solution using the 10 and 15 μm particles as displayed in Fig. 4b. These unusual particle-focusing behaviors can be used to develop an efficient particle sorter without employing any complex geometry.

From these experimental results, it was found that the large particles were more primarily affected by the sign of N_1 than the small particles, resulting in the close-wall double-line particle focusing. On the other hand, the small particles were focused at the center. The experimental observation can be explained with the help of the following assumption: the particle focusing is determined by the normal stress components themselves but not their differences. That is, when $N_1 < 0$ at high El values, the larger particles are focused along double lines close to the side wall than the smaller particles. For the viscoelastic fluids with $N_1 > 0$, all the particles, however, are focused at the center (see Fig. 3a).

The difference between the first and the second normal-stress differences ($\Delta N = N_1 - N_2$) was measured using a rheometer with 50-mm-diameter parallel plates to figure out how the particle focusing is affected by τ_{yy}, as shown in Fig. 5a. Since the HPC and PEO solutions are non-linear viscoelastic solutions, the exact values of the normal stress components (e.g., τ_{xx}, τ_{yy} and τ_{zz}) cannot be obtained by mathematical calculation or measurement. Based on the N_1 and ΔN results, we hypothesize that the τ_{yy} acting on the particles in the HPC solutions has higher values than those of PEO solutions. We first confirmed the rheological properties of diluted HPC solutions in which the viscosities are very low and shear thinning behaviors are minor in comparison with those of diluted PEO solutions. For example, the viscosity and power law index of 100 ppm HPC solution is around 1.9 mPa·s and 0.9864, respectively (Fig. 5b and Table 1). Upon the flow conditions conducted in our experiment in Fig. 3b, the 100 ppm HPC solution has $El = 0.189$ and $Re = 0.412$, representing that the solution is in the regime of very weakly elastic with negligible shear thinning and inertia-free. In such a condition, particles in PEO solutions with positive normal stress difference tend to be randomly distributed, which is totally different from our results. In previous report, Liu et al. showed the double-line particle focusing of large particles and the center-focusing of small particles using dilute PEO solutions. However, the flow conditions in their work are highly elastic ($El = 8.8$–140.7) and inertial forces are not negligible ($Re = 1.39$–5.56) in which shear rate dependency, inertia, and elasticity become important. In our experiment, we revealed that particles under very low $El = 0.189$ and $Re = 0.412$ in the 100 ppm HPC solution migrate towards the channel side walls not by the shear rate dependency nor the inertia, but by the normal stress difference that is divided into two normal stress components, τ_{xx} and τ_{yy}. Between them, τ_{yy} is mainly related with the lateral particle migration. We may conclude by observing them that the stress component τ_{yy} is a crucial factor for a particle lateral migration in the first normal stress difference N_1. In line with this viewpoint, the τ_{yy} increases as increasing the concentrations of the HPC solutions. We argue that the particle focusing behavior can be explained by the normal stress components τ_{xx} and τ_{yy} by which the particles can migrate along the lateral direction to the flow.

Based on the experimental results, a possible particle focusing mechanism in viscoelastic fluids with the positive and negative N_1 was suggested (Fig. 6). The inertial forces including the shear-gradient lift force (F_{LS}) and wall-repulsion force (F_{WS}), and the elastic force (F_E) are developed in the microfluidic channel. In many cases, the inertial forces are negligible due to low Re. In Fig. 6, the elastic forces developed by τ_{xx} and τ_{yy} are expressed as $F_{E,\,\tau_{xx}}$ and $F_{E,\,\tau_{yy}}$, respectively. For typical viscoelastic fluids, the shear stress (τ_{xy}) and the normal stress (τ_{xx}), which are functions of the shear rate, become stronger at the channel walls than the channel center (Fig. 6). The strong formation of the τ_{xx} and τ_{xy} at the channel walls causes the lateral particle migration towards the centerline. In many polymer solutions such as diluted PEO solutions, the τ_{yy} is relatively small (i.e., negligible $F_{E,\,\tau_{yy}}$). Hence, the only driving force for the lateral particle migration is the τ_{xx} and τ_{xy}, which results in the particle focusing to the center (Fig. 6a). However, since the diluted HPC solution has a remarkably large $F_{E,\,\tau_{yy}}$, the particle movement is affected by not only the τ_{xx} and τ_{xy} but also by the τ_{yy} (Fig. 6b). Consequently, the particles are double-line focused close to the channel walls when $F_{E,\,\tau_{yy}}$ is larger than $F_{E,\,\tau_{xx}} + F_v$. Here, F_v is the viscous drag force that resists the lateral migration of particles. Previously, Nam *et al*. explored a particle focusing mechanism using the elasto-inertial focusing principle and categorized the direction of forces acting on the particle (Nam et al. 2012) under the positive first normal stress difference flow. It was reported that the wall-repulsion force pushes the particle against counteracting forces, in our case τ_{yy} multiplied by a hemisphere surface area of the particle. Overall, the combination of the forces acting on the particle allows the particle to be focused in between the centerline and channel walls.

These experimental results imply that the suspended particles in the diluted HPC solution are subject to the larger

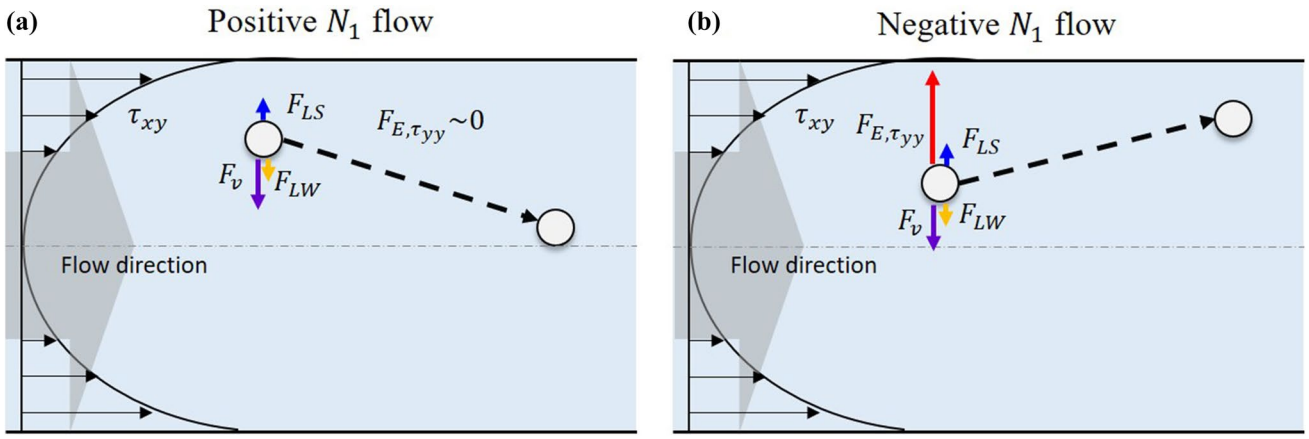

Fig. 6 Schematic illustration of the focusing mechanism of a particle in viscoelastic fluids. **a** Particle behavior in the positive N_1 flow. The particle is focused at the center when the τ_{yy} is negligible. **b** Particle behavior in the negative N_1 flow. The particle is double-line focused close to the wall when the $F_{E,\tau_{yy}}$ outweighs the $F_{\tau_{xy}} + F_{E,\tau_{xx}}$. Here $F_{E,\tau_{xx}}$ and $F_{E,\tau_{yy}}$ are the elastic forces from $\tau_{xx}$and τ_{yy}, respectively, and F_v is viscous force from τ_{xy}

normal force than the less viscous drag force, thus resulting in the peculiar particle migration. On the other hand, the effect of particle sizes on the normal force τ_{yy} for the lateral particle migration is not obvious in the diluted PEO solutions, which leads to the centerline-focusing of particles. The large particles in the HPC solution were double-line focused in all the cases, while the small particles were either focused at the center or close to the wall depending on the negative N_1 values. When the τ_{xx} is dominant, *e.g.*, the PEO solution with the positive N_1, the particles can be focused at the center. When the contribution of τ_{yy} becomes more significant than $\tau_{xx} - \tau_{yy}$ in such a case of the diluted HPC solution, different particle focusing behavior occurs. These results indicate that the N_1 variation can serve as an effective indicator to understand the reversed particle-focusing phenomenon.

4 Conclusions

In this study, we investigated the lateral particle migration in viscoelastic fluids with the positive or negative N_1. The corresponding particle focusing mechanism was analyzed by altering polymer concentrations and particle sizes suspended in the solutions. We harnessed the normal stress components τ_{xx} and $\tau_{yy}$to explain the possible mechanism of the particle migration behaviors in the viscoelastic fluids with positive and negative N_1. The viscoelastic solutions with the negative N_1 showed a reversed particle-focusing phenomenon compared with those with the positive N_1, which indicated that τ_{yy} plays a significant role in the particle migration. It is anticipated that the reverse particle-focusing based on the negative normal stress difference could be applied to a new type of flow cytometry which is able to separate and focus particles with different sizes in viscoelastic fluids.

Acknowledgements The authors acknowledge the support from the soft chemical materials research center for organic–inorganic multi-dimensional structure, which is funded by Gyeonggi Regional Research center Program (GRRC Dankook 2016-B03). Also, it was supported by the Industrial Strategic Technology Development Program, which is funded by the Ministry of Trade, Industry and Energy (MI, Korea) [10052641]. The authors are grateful for these supports.

References

Acad JEANY (1984) Optical properties of hydroxypropyl cellulose. Macromolecules 17:1512–1520. https://doi.org/10.1021/ma00138a016

Ahn SW, Lee SS, Lee SJ, Kim JM (2015) Microfluidic particle separator utilizing sheathless elasto-inertial focusing. Chem Eng Sci 126:237–243. https://doi.org/10.1016/j.ces.2014.12.019

Barnes HA (1989) An introduction to rheology. Elsevier, Amsterdam

Cartas-Ayala MA, Raafat M, Karnik R (2013) Self-sorting of deformable particles in an asynchronous logic microfluidic circuit. Small 9:375–381. https://doi.org/10.1002/smll.201201422

Cha S, Shin T, Lee SS et al (2012) Cell stretching measurement utilizing viscoelastic particle focusing. Anal Chem 84:10471–10477. https://doi.org/10.1021/ac302763n

D'Avino G, Romeo G, Villone MM et al (2012) Single line particle focusing induced by viscoelasticity of the suspending liquid: theory, experiments and simulations to design a micropipe flow-focuser. Lab Chip 12:1638. https://doi.org/10.1039/c2lc21154h

Del Giudice F, Romeo G, D'Avino G et al (2013) Particle alignment in a viscoelastic liquid flowing in a square-shaped microchannel. Lab Chip 13:4263–4271. https://doi.org/10.1039/c3lc50679g

Del Giudice F, D'Avino G, Greco F et al (2015a) Effect of fluid rheology on particle migration in a square-shaped microchannel. Microfluid Nanofluidics 19:95–104. https://doi.org/10.1007/s10404-015-1552-x

Del Giudice F, D'Avino G, Greco F et al (2015b) Rheometry-on-a-chip: measuring the relaxation time of a viscoelastic liquid through

particle migration in microchannel flows. Lab Chip 15:783–792. https://doi.org/10.1039/C4LC01157K
Eom Y, Jung D, Hwang SS, Kim B (2016) Characteristic dynamic rheological responses of nematic poly(p-phenylene terephthalamide) and cholesteric hydroxypropyl cellulose phases. Polym J 48:869–874. https://doi.org/10.1038/pj.2016.46
Fried F, Leal CR, Godinho MH, Martins AF (1994) The first normal stress difference and viscosity in shear of liquid crystalline solutions of hydroxypropylcellulose: new experimental data and theory. Polym Adv Technol 5:596–599. https://doi.org/10.1002/pat.1994.220050922
Guan G, Wu L, Bhagat AA et al (2013) Spiral microchannel with rectangular and trapezoidal cross-sections for size based particle separation. Sci Rep 3:1475. https://doi.org/10.1038/srep01475
Ho BP, Leal LG (1976) Migration of rigid spheres in a two-dimensional unidirectional shear flow of a second-order fluid. J Fluid Mech 76:783. https://doi.org/10.1017/S002211207600089X
Hoekstra H, Vermant J, Mewis J, Narayanan T (2002) Rheology and structure of suspensions in liquid crystalline hydroxypropylcellulose solutions. Langmuir 18:5695–5703. https://doi.org/10.1021/la020097y
Hongladarom K, Secakusuma V, Burghardt WR (1994) Relation between molecular orientation and rheology in lyotropic hydroxypropylcellulose solutions. J Rheol (N Y N Y) 38:1505–1523. https://doi.org/10.1122/1.550556
Howard MP, Panagiotopoulos AZ, Nikoubashman A (2015) Inertial and viscoelastic forces on rigid colloids in microfluidic channels. J Chem Phys. https://doi.org/10.1063/1.4922323
Huang PY, Feng J, Hu HH, Joseph DD (1997) Direct simulation of the motion of solid particles in Couette and Poiseuille flows of viscoelastic fluids. J Fluid Mech 343:S0022112097005764. https://doi.org/10.1017/S0022112097005764
Janmey PA, McCormick ME, Rammensee S et al (2007) Negative normal stress in semiflexible biopolymer gels. Nat Mater 6:48–51. https://doi.org/10.1038/nmat1810
Kang AR, Ahn SW, Lee SJ et al (2011) Medium viscoelastic effect on particle segregation in concentrated suspensions under rectangular microchannel flows. Korea Aust Rheol J 23:247–254. https://doi.org/10.1007/s13367-011-0030-6
Kang K, Lee SS, Hyun K et al (2013) DNA-based highly tunable particle focuser. Nat Commun 4:2567. https://doi.org/10.1038/ncomms3567
Kharchenko SB, Douglas JF, Obrzut J et al (2004) Flow-induced properties of nanotube-filled polymer materials. Nat Mater 3:564–568. https://doi.org/10.1038/nmat1183
Kim B, Kim JM (2016) Elasto-inertial particle focusing under the viscoelastic flow of DNA solution in a square channel. Biomicrofluidics. https://doi.org/10.1063/1.4944628
Kim J, Kim JY, Kim Y et al (2017) Shape measurement of ellipsoidal particles in a cross-slot microchannel utilizing viscoelastic particle focusing. Anal Chem 89:8662–8666. https://doi.org/10.1021/acs.analchem.7b02559
Kiss G, Porter RS (1980) Rheology of concentrated solutions of helical polypeptides. J Polym Sci Polym Phys Ed 18:361–388. https://doi.org/10.1002/pol.1980.180180217
Korneeva EV, Shtennikova IN, Shibaev VP et al (1990) Conformational properties of hydroxypropylcellulose !. Hydrodynamic properties and equilibrium rigidity of its macromolecules. Eur Polym J 26:781–785
Kulichikhin VG, Makarova VV, Tolstykh MY et al (2011) Structural evolution of liquid-crystalline solutions of hydroxypropyl cellulose and hydroxypropyl cellulose-based nanocomposites during flow. Polym Sci Ser A 53:748–764. https://doi.org/10.1134/S0965545x11090070 doi
Larson RG (1990) Arrested Tumbling in shearing flows of liquid crystal polymers. Macromolecules. https://doi.org/10.1021/ma00219a020
Lee DJ, Brenner H, Youn JR, Song YS (2013) Multiplex particle focusing via hydrodynamic force in viscoelastic fluids. Sci Rep 3:3258. https://doi.org/10.1038/srep03258
Leshansky AM, Bransky A, Korin N, Dinnar U (2007) Tunable nonlinear viscoelastic "focusing" in a microfluidic device. Phys Rev Lett. https://doi.org/10.1103/PhysRevLett.98.234501
Li G, McKinley GH, Ardekani AM (2015) Dynamics of particle migration in channel flow of viscoelastic fluids. J Fluid Mech 785:486–505. https://doi.org/10.1017/jfm.2015.619
Li D, Lu X, Xuan X (2016) Viscoelastic separation of particles by size in straight rectangular microchannels: a parametric study for a refined understanding. Anal Chem. https://doi.org/10.1021/acs.analchem.6b03501
Lim EJ, Ober TJ, Edd JF et al (2014a) Inertio-elastic focusing of bioparticles in microchannels at high throughput. Nat Commun 5:4120. https://doi.org/10.1038/ncomms5120
Lim H, Nam J, Shin S (2014b) Lateral migration of particles suspended in viscoelastic fluids in a microchannel flow. Microfluid Nanofluidics 17:683–692. https://doi.org/10.1007/s10404-014-1353-7
Lin-Gibson S, Pathak JA, Grulke EA et al (2004) Elastic Flow Instability in nanotube suspensions. Phys Rev Lett 92:048302. https://doi.org/10.1103/PhysRevLett.92.048302
Liu C, Xue C, Hu G (2015) Sheathless separation of particles and cells by viscoelastic effects in straight rectangular microchannels. Proc Eng 126:721–724. https://doi.org/10.1016/j.proeng.2015.11.278
Lu X, Xuan X (2015) Elasto-inertial pinched flow fractionation for continuous shape-based particle separation. Anal Chem 87:11523–11530. https://doi.org/10.1021/acs.analchem.5b03321
Lu X, Zhu L, Hua R, Xuan X (2015) Continuous sheath-free separation of particles by shape in viscoelastic fluids. Appl Phys Lett. https://doi.org/10.1063/1.4939267
Martins AF, Leal CR, Godinho MH, Fried F (2001) The influence of polymer molecular weight on the first normal-stress difference and shear-viscosity of LC solutions of hydroxypropylcellulose. Mol Cryst Liq Cryst 362:305–312. https://doi.org/10.1080/10587250108025777 doi
Miller MJ, Christiansen EB (1972) The stress state of elastic fluids in viscometric flow. AIChE J 18:600–608. https://doi.org/10.1002/aic.690180321
Morrison F (2001) Understanding rheology. Oxford Univ Press, Oxford. https://doi.org/10.3933/ApplRheol-12-233
Nam J, Lim H, Kim D et al (2012) Continuous separation of microparticles in a microfluidic channel via the elasto-inertial effect of non-Newtonian fluid. Lab Chip. https://doi.org/10.1039/c2lc21304d
Nam J, Tan JKS, Khoo BL et al (2015) Hybrid capillary-inserted microfluidic device for sheathless particle focusing and separation in viscoelastic flow. Biomicrofluidics 9:064117. https://doi.org/10.1063/1.4938389
Pasquali M (2004) Swell properties and swift processing. Nat Mater 3:509–510. https://doi.org/10.1038/nmat1188
Phillies GDJ, O'Connell R, Whitford P, Streletzky KA (2003) Mode structure of diffusive transport in hydroxypropyl cellulose: Water. J Chem Phys 119:9903–9913. https://doi.org/10.1063/1.1615968
Procedures E (1990) Conformational properties of hydroxypropylcellulose–ii. flow birefringence and optical anisotropy of hydroxypropylcellulose macromolecules. Eur Polym J 26:787–790
Romeo G, D'Avino G, Greco F et al (2013) Viscoelastic flow-focusing in microchannels: scaling properties of the particle radial distributions. Lab Chip 13:2802. https://doi.org/10.1039/c3lc50257k
Shaw MT, MacKnight WJ (2005) Introduction to polymer viscoelasticity, 3rd edn. John Wiley & Sons, Hoboken, United States

Tian F, Zhang W, Cai L et al (2017) Microfluidic co-flow of Newtonian and viscoelastic fluids for high-resolution separation of microparticles. Lab Chip. https://doi.org/10.1039/C7LC00671C

Villone MM, D'Avino G, Hulsen MA et al (2011) Simulations of viscoelasticity-induced focusing of particles in pressure-driven micro-slit flow. J Nonnewton Fluid Mech 166:1396–1405. https://doi.org/10.1016/j.jnnfm.2011.09.003

Villone MM, D'Avino G, Hulsen MA et al (2013) Particle motion in square channel flow of a viscoelastic liquid: migration vs. secondary flows. J Nonnewton Fluid Mech 195:1–8. https://doi.org/10.1016/j.jnnfm.2012.12.006

Yang S, Kim JY, Lee SJ et al (2011) Sheathless elasto-inertial particle focusing and continuous separation in a straight rectangular microchannel. Lab Chip 11:266–273. https://doi.org/10.1039/c0lc00102c

Yang SH, Lee DJ, Youn JR, Song YS (2017) Multiple-line particle focusing under viscoelastic flow in a microfluidic device. Anal Chem 89:3639–3647. https://doi.org/10.1021/acs.analchem.6b05052

Young Kim J, Won Ahn S, Sik Lee S, Min Kim J (2012) Lateral migration and focusing of colloidal particles and DNA molecules under viscoelastic flow. Lab Chip 12:2807. https://doi.org/10.1039/c2lc40147a

Yuan D, Zhang J, Yan S et al (2015) Dean-flow-coupled elasto-inertial three-dimensional particle focusing under viscoelastic flow in a straight channel with asymmetrical expansion–contraction cavity arrays. Biomicrofluidics. https://doi.org/10.1063/1.4927494